Micelle Formation of a Rod−Coil Diblock Copolymer in a Solvent Selective for the Rod Block

Jin Wu, Eli M. Pearce,* and T. K. Kwei

Department of Chemical Engineering and Chemistry, Herman F. Mark Polymer Research Institute, Polytechnic University, 6 MetroTech Center, Brooklyn, New York 11201

Amy A. Lefebvre and Nitash P. Balsara*

Department of Chemical Engineering, University of California, Berkeley, California 94720, and Materials Science Division, Lawrence Berkeley National Laboratory, University of California, Berkeley, California 94720

Received August 20, 2001

ABSTRACT: Aggregation of an amphiphilic rod−coil diblock copolymer, poly(*n*-hexyl isocyanate)-*b*-poly(ethylene glycol) (PHIC-*b*-PEG), in toluene, a selective solvent for the rodlike PHIC block, was studied using light scattering and polarized optical microscopy. Static and dynamic light scattering data indicate the formation of cylindrical micelles with a hydrodynamic radius of 279 nm in very dilute solutions (weight fraction of polymer, *w*, from 0.0002 to 0.008) at 25 °C. The cylindrical micelles were determined to be disklike (planar), 0.9 μm in diameter and 20 nm in thickness, based on a comparison between the experimental data and the theory of scattering and self-diffusion of ellipsoids. Planar aggregates are expected if nematic interactions of the coronal rod block are dominant. The aggregate size decreases with increasing temperature. The micelles were observed visually in solution with the help of a polarized optical microscope due to the optical anisotropy of the PHIC block. Disklike objects with diameters in the micron range were observed to undergo translational and rotational motion in and out of the focal plane of the microscope.

Introduction

The self-assembly and phase behavior of rod−coil block copolymers have attracted considerable attention.[1−6] Theoretical studies predict that the self-assembly characteristics of these molecules in selective solvents would differ considerably from those of conventional coil−coil block copolymers.[7−12] Aggregation of rod−coil block copolymers is driven by both the selectivity of the solvent and the liquid crystalline character of one of the blocks.

Some experiments on aggregation of rod−coil block copolymers in solvents that are selective toward the rod block have been conducted. Jenekhe and Chen[1] observed that amphiphilic poly(phenylquinoline)-*b*-polystyrene rod−coil block copolymers self-organized into spherical, vesicular, cylindrical, and lamellar aggregates with micron dimensions. The sizes of the aggregates were about 2 orders of magnitude larger than those in coil−coil block copolymers. Moreover, solution cast micellar films were iridescent due to long-range ordering of the micelles.[1] In another study,[2] micelle formation of charged polystyrene-*b*-poly(isocyanodipeptide) rod−coil block copolymers in aqueous media was studied. The morphology of the aggregates was controlled by varying the length of the rigid-rod block, pH, and anion−headgroup interactions. In these experiments,[1,2] the aggregation was observed by microscopy of dry samples after the solvent was removed. The theories on aggregation of rod−coil block copolymers[7−12] are restricted to solvents that are selective toward the coil block and are thus not applicable to these experiments.[1,2]

In this paper, we study aggregation of a poly(*n*-hexyl isocyanate)-*b*-poly(ethylene glycol) copolymer (PHIC-*b*-PEG). PHIC chains adopt a 12_5 helical structure[13] and are relatively stiff in a wide range of solvents such as toluene and chloroform.[14,15] The stiffness of PHIC is primarily due to short-range restrictions to rotation and is characterized by a persistence length of 50−60 nm. The chain stiffness leads to interesting effects such as thermoreversible aggregation and gelation in PHIC solutions.[16] Like previous studies on rod−coil block copolymers,[1,2] the solvent used in this study, toluene, is a good solvent for the rod (PHIC) block but a poor solvent for the coil (PEG) block. The aggregation behavior of PHIC-*b*-PEG in toluene solutions is studied by static and dynamic light scattering. We also demonstrate that direct visualization of the aggregates in solution is possible by polarized optical microscopy due to the optical anisotropy of PHIC.[17]

Experimental Section

Materials. The methods used to synthesize, characterize, and isolate the PHIC-*b*-PEG diblock copolymer used in this study are described in ref 18. The chemical structure is shown in Figure 1. The weight-averaged number of repeating units for the PHIC and PEG blocks was 50 and 12, respectively. The polydispersity index of the copolymer was 1.20. HPLC grade toluene was used to prepare the solutions in this study.

Dynamic and Static Light Scattering. The PHIC-*b*-PEG/toluene solutions were made by adding filtered toluene to the polymer. The solutions (without further filtration) were annealed at 60 °C for 48 h and then cooled to room temperature to allow equilibrium to be reached. Solutions are identified by the weight fraction of polymer, *w*. Samples with *w* ranging between 0.0002 and 0.05 were studied. The measured characteristics of the PHIC-*b*-PEG/toluene solutions in the temperature range of interest were independent of history after annealing. This is a necessary (but not sufficient) condition for establishing equilibrium. Static and dynamic light scattering (SLS and DLS, respectively) studies were performed at 25 and 40 °C using an ALV-5000 instrument with a 100 mW solid-state frequency-doubled Nd:YAG laser ($\lambda = 532$ nm) as

10.1021/ma011502f CCC: $22.00
Published on Web 01/26/2002

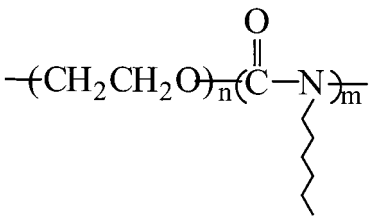

Figure 1. Chemical structure of the synthetic rod−coil diblock copolymer, poly(*n*-hexyl isocyanate)-*b*-poly(ethylene glycol) (PHIC-*b*-PEG).

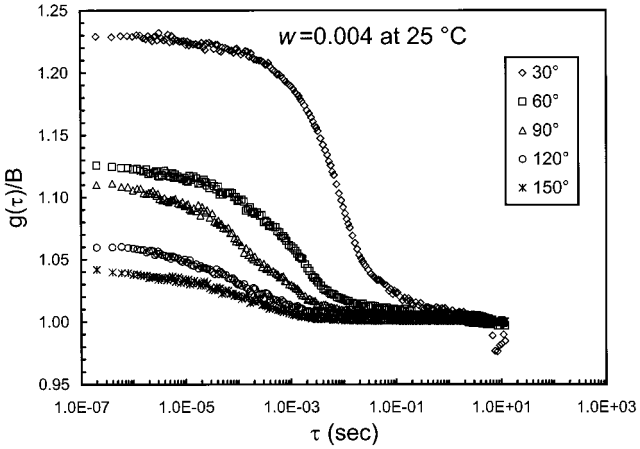

Figure 2. Normalized autocorrelation functions obtained from the PHIC-*b*-PEG/toluene solution ($w = 0.004$, 25 °C) at various scattering angles.

the incident source. Data were obtained at several scattering angles between 30° and 150°. The SLS signals were converted to absolute intensities $I(q)$ using pure toluene as a secondary standard. The time autocorrelation function of the scattered intensity $g(\tau)$ was accumulated in the homodyne mode and used to obtain the intensity-weighed distribution of mobilities $G(\Gamma)$ by solving the integral eq 1:[19,20]

$$g(\tau) = B[\alpha\{\int_0^\infty G(\Gamma)\exp(-\Gamma\tau)d\Gamma\}^2 + 1] \qquad (1)$$

The solution was obtained using the CONTIN software package developed by Provencher.[21] In most of the data sets, the distribution of mobilities was dominated by a single broad relaxation mode. This mode was seen consistently in all of the data, and we report the characteristic decay rate associated with this relaxation mode (Γ_c), given by the ratio of the first and zeroth moments of the peak. A very slow relaxation mode (well separated from Γ_c) was seen in some of the data sets, particularly those at the lowest scattering angle ($\theta = 30°$). We attribute the slow mode to the presence of dust; we did not filter our polymer solutions because we were unsure of the effect of filtration on the aggregates that form in solution. At the lowest scattering angle (30°), the dust signal contribution ranged between 30% and 50% of the total signal.

Polarized Optical Microscopy (POM). The morphologies of the aggregates in dilute PHIC-*b*-PEG/toluene solutions were observed using a Nikon Optiphot polarized optical microscope (bright field, crossed polarizer, and 300-fold magnification) with a Nikon FX-35A camera at room temperature. A homemade glass liquid cell was used in this study with a 5 mm deep hole and a thin glass cover.

Results and Discussion

We begin by discussing results obtained in PHIC-*b*-PEG/toluene solutions with w less than 0.01. Typical DLS data obtained from these dilute solutions are shown in Figure 2 where we show data from the $w = 0.004$ solution at 25 °C. The dependence of Γ_c on q^2 [$q = 4\pi n \sin(\theta/2)/\lambda$, where θ is the scattering angle, n is the refractive index of the solution, and λ is the wavelength of the incident beam] is shown in Figure 3. Within experimental error, Γ_c at a given q is independent of concentration. The relaxation mode identified in the dilute solutions is thus approximately diffusive with an apparent diffusion coefficient (given by the slope of the Γ_c vs q^2 plot) of 1.4×10^{-8} cm^2/s. Because of the concentration independence of the relaxation mode, we assume that this corresponds to the self-diffusion coefficient of the PHIC-*b*-PEG aggregates in solution (D_0). The Stokes−Einstein relationship is then used to estimate the hydrodynamic radius (R_h) of the diffusing aggregates:

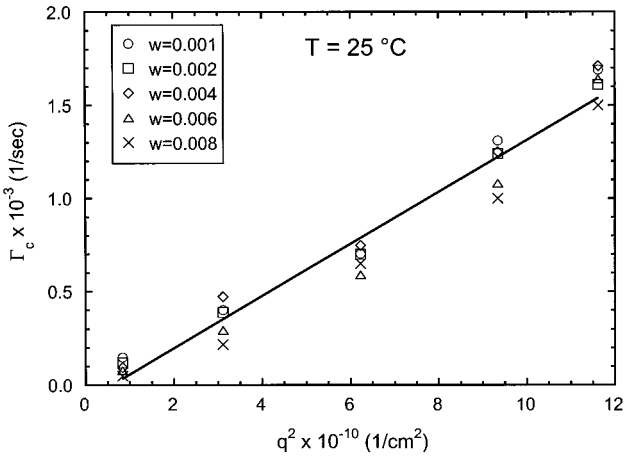

Figure 3. The q^2 dependence of Γ_c for PHIC-*b*-PEG/toluene solutions of various concentrations ($w < 0.01$) at 25 °C. The solid line is the least-squares linear fit through all of the data. The slope of the line (1.4×10^{-8} cm^2/s) is the apparent diffusion coefficient.

$$D_0 = \frac{k_B T}{6\pi\eta_0 R_h} \qquad (2)$$

where k_B is the Boltzmann constant, T is the absolute temperature, and η_0 is the viscosity of the solvent at T. The average hydrodynamic size of the diffusing species R_h thus obtained is 279 nm [η_0(25 °C) = 0.558 cps].

The fully extended length of this PHIC-*b*-PEG copolymer is calculated to be only around 12 nm as follows. The fully extended length of the PEG block (12 repeating units) is around 3 nm, using 0.154 nm as the C−C bond length, 0.143 nm as the C−O bond length, and 108° as the C−C−O bond angle. For the rigid-rod PHIC block, the translation per monomer of poly(*n*-alkyl isocyanate) was reported to be in the range of 1.8−2.0 Å from X-ray[22] and light scattering[23,24] data. Thus, the length of the PHIC block (50 repeating units) is estimated to be around 9 nm.

The large disparity between R_h (279 nm) and the length of the fully extended PHIC-*b*-PEG molecule (12 nm) rules out the possibility of spherical micelles. We thus examine the possibility of the micelles being ellipsoids of revolution.[25−27] The hydrodynamic radius of ellipsoids obtained by revolving an ellipse with semiaxes a and b about the a axis was obtained by Perrin.[28] The results of Perrin are given in eqs 3−5:

$$R_h = \frac{a}{f\left(\frac{b}{a}\right)} \qquad (3)$$

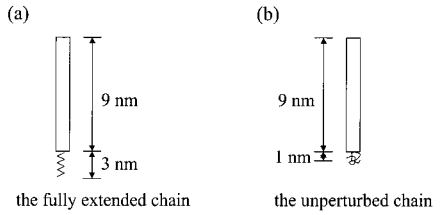

Figure 4. Estimated chain length of the PHIC-*b*-PEG molecule with the PEG block (a) fully extended and (b) unperturbed.

Table 1. Dimensions of Ellipsoidal Particles That Yield a Hydrodynamic Radius of 279 nm Based on Perrin's Theory[28]

minor semiaxis (nm)	major semiaxis (nm)		radius of sphere (nm)
	prolate	oblate	
10	1611	432	279

For prolate ellipsoids ($a > b$),

$$f(b/a) = \frac{\ln\left[\frac{1 + \sqrt{1 - b^2/a^2}}{b/a}\right]}{\sqrt{1 - b^2/a^2}} \quad (4)$$

While for oblate ellipsoids ($a < b$),

$$f(b/a) = \frac{\tan^{-1}[\sqrt{b^2/a^2 - 1}]}{\sqrt{b^2/a^2 - 1}} \quad (5)$$

For micellar aggregates, the minor semiaxis is restricted to molecular dimensions. Since the rigid-rod block does not have conformational degrees of freedom, the lower bound for the minor semiaxis is 10 nm (9 nm for the PHIC chain and 1 nm for the unperturbed PEG chain), and the upper bound is 12 nm (9 nm for the PHIC chain and 3 nm for the fully extended PEG chain) (Figure 4). These values are much smaller than the value of R_h of the micelles. The exact amount of chain stretching of the PEG block has negligible effect on the computed scattering characteristics of the micelles. For simplicity, we assume a value of 10 nm for the minor semiaxis. Using this constraint, we use eqs 4 and 5 to find the values of the major semiaxes of prolate and oblate ellipsoids that would yield $R_h = 279$ nm. The dimensions of the ellipsoidal particles thus obtained are given in Table 1. For prolate ellipsoids, the major semiaxis is estimated to be 1611 nm. For the oblate ellipsoids, the major semiaxis is estimated to be 432 nm. The large disparity between a and b for both cases indicates that the micelles are, to a very good approximation, either rodlike (1-dimensional) or disklike (2-dimensional). The DLS data from anisotropic micron-sized objects in the accessible q range may contain additional contributions due to the flexibility of the aggregates. This may be the reason for the fact that the Γ_c vs q^2 plot does not go through the origin (Figure 3).

In Figure 5 we show the DLS data from dilute PHIC-*b*-PEG/toluene solutions at 40 °C. The data are qualitatively similar to those obtained at 25 °C. The slope of the Γ_c vs q^2 plot is determined to be 2.0×10^{-8} cm^2/s with a corresponding R_h of 232 nm [η_0(40 °C) = 0.471 cps]. The aggregates are thus 20% smaller at 40 °C than they were at 25 °C.

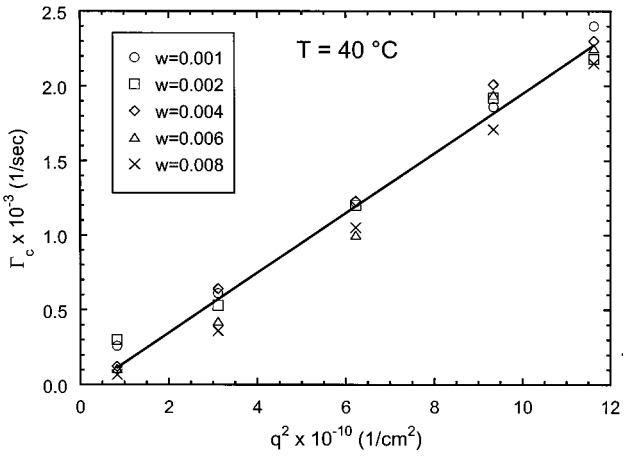

Figure 5. The q^2 dependence of Γ_c for PHIC-*b*-PEG/toluene solutions of various concentrations ($w < 0.01$) at 40 °C. The solid line is the least-squares linear fit through all of the data. The slope of the line (2.0×10^{-8} cm^2/s) is the apparent diffusion coefficient.

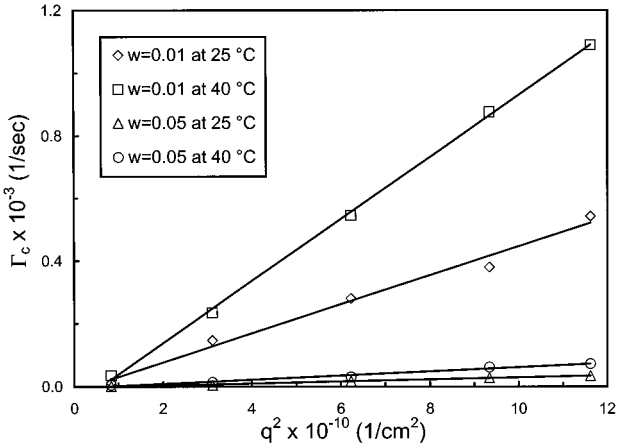

Figure 6. The q^2 dependence of Γ_c for PHIC-*b*-PEG/toluene solutions of various concentrations ($w \geq 0.01$) at 25 and 40 °C. The solid lines are least-squares linear fits through the data.

The DLS data at relatively high concentrations ($w = 0.01$ and 0.05) are shown in Figure 6 where we plot Γ_c vs q^2. We see a distinct decrease in the apparent diffusion coefficient ($D_{app} = \Gamma_c/q^2$) with increasing concentration. The concentration dependence of D_{app} at 25 and 40 °C is shown in Figure 7. The sharp decrease in D_{app} seen at $w = 0.01$ indicates an abrupt change in the structure of the solution. This may be due to an abrupt change in the structure of the micelle or the organization of the micelles into a weakly ordered state. Resolution between these two possibilities will be presented shortly.

Static light scattering measurements were performed in the concentration regime of $w < 0.01$ at 25 °C to determine the structure of the micelle. The q dependence of the scattered intensity $I(q)$ is shown in Figure 8 where we plot the concentration-normalized scattered intensity $I(q)/w$. As can be seen from Figure 8, the data from all of the solutions collapse to a single curve, which indicates that the size and shape of the aggregates do not change within the concentration range studied. This is consistent with the DLS results. For both the possible aggregates that we consider (oblate and prolate ellipsoids), the q range of our instrument is such that $qL > 1$, where L is the characteristic size of the aggregate.

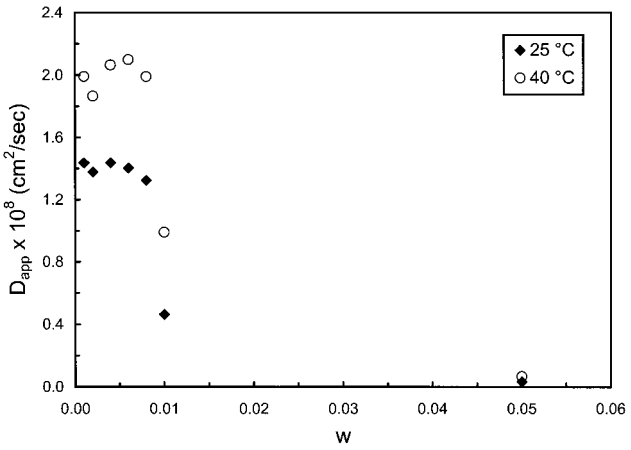

Figure 7. Dependence of the apparent diffusion coefficient on the weight fraction of PHIC-*b*-PEG in toluene at 25 and 40 °C.

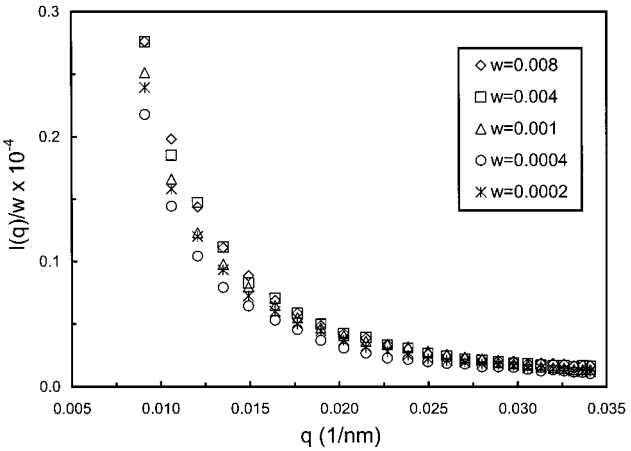

Figure 8. The *q* dependence of SLS intensity normalized by the weight fraction of PHIC-*b*-PEG in toluene, $I(q)/w$, at 25 °C.

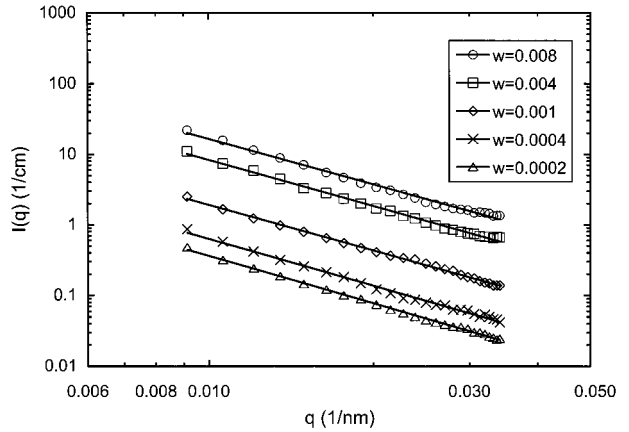

Figure 9. A log−log plot of the SLS intensity vs *q* for PHIC-*b*-PEG/toluene solutions of various concentrations ($w < 0.01$) at 25 °C. The solid lines are power law fits through the data.

In this *q* regime, the fractal dimension of the aggregate can be obtained from the slope of the log(I) vs log(q) plot. The plots of log(I) vs log(q) for each solution are shown in Figure 9. The lines through the data in Figure 9 are power law fits with slopes ranging between 2.15 and 2.22. It is thus clear that the aggregates are approximately two-dimensional, i.e., disklike. SLS measurements performed at 40 °C give similar results and are not shown.

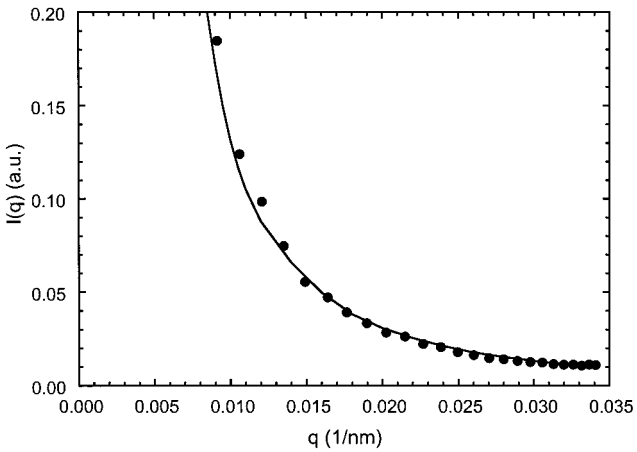

Figure 10. The *q* dependence of the SLS intensity of the $w = 0.004$ PHIC-*b*-PEG/toluene solution at 25 °C. The solid line through the data is the theoretical scattering profile for an oblate ellipsoid with yields $R_h = 279$ nm.

The static scattering intensity $I(q)$ of a solution of randomly oriented ellipsoids is given by eqs 6−8:

$$I(q) = \frac{9\pi}{2}\int_0^{\pi/2}\frac{[J_{3/2}(u)]^2}{u^3}\cos\beta\,\mathrm{d}\beta \tag{6}$$

where

$$u = qa\sqrt{\cos^2\beta + \frac{b^2}{a^2}\sin^2\beta} \tag{7}$$

and $J_{3/2}(u)$ is the $^3/_2$-order Bessel function:

$$J_{3/2}(u) = \sqrt{\frac{2u}{\pi}}\left(\frac{\sin u}{u^2} - \frac{\cos u}{u}\right) \tag{8}$$

The theoretical $I(q)$ for oblate ellipsoids with $a = 10$ nm and $b = 432$ nm was computed using eqs 6−8, and the resulting curve is compared with the experimental data from the $w = 0.004$ solution in Figure 10. The experimental curve was multiplied by 0.017 to obtain the best agreement between theory and experiment. We have chosen to show only one experimental data set in Figure 10, since all of the experimental curves can be superimposed by the use of scaling factors. It is evident in Figure 10 that the measured static scattering profile is consistent with the computed scattering profile, using parameters obtained independently from DLS. We note that the computed $I(q)$ of the other structures in Table 1 are qualitatively inconsistent with the measured data. This confirms the disklike nature of the PHIC-*b*-PEG aggregates in toluene.

It is important to note that our analysis of the scattering data is based on a highly simplified model of the micellar aggregates. We assume that the aggregates are monodisperse, homogeneous, rigid, oblate ellipsoids. In reality, micellar aggregates are polydisperse,[29] inhomogeneous, and flexible. It is likely that the lack of quantitative agreement between the model and experiments (e.g., finite intercept seen in Figures 3, 5, and 6) is due to the simplicity of our analysis.

We now return to the abrupt change in D_{app} noted at $w = 0.01$ in Figure 7. For disks with radius R and thickness d, an isotropic-to-nematic transition is expected when spheres swept by adjacent disks overlap.[30] We thus expect organization of the disklike micelles

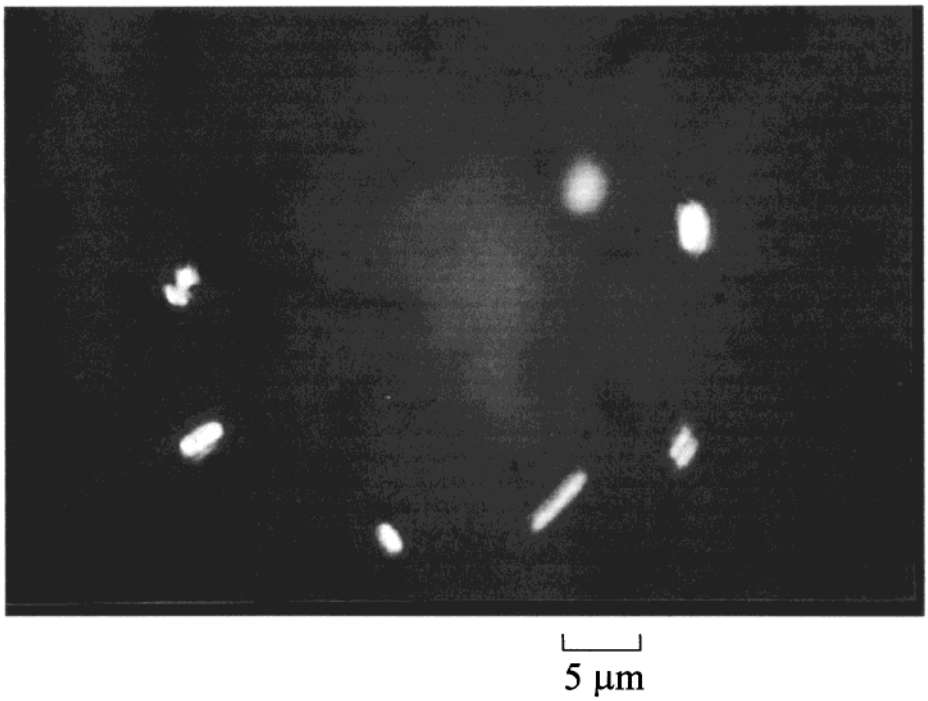

Figure 11. Polarized optical micrograph of the cylindrical aggregates formed from the PHIC-*b*-PEG/toluene solution ($w = 0.004$) at room temperature.

when their volume fraction ϕ exceeds $3d/4R$. Substituting $d = 10$ nm and $R = 432$ nm, we obtain $\phi = 0.017$. This compares well with the concentration at which the abrupt change in D_{app} was noted (Figure 7). We thus conclude that diffusion in solutions with $w > 0.01$ is slow due to the organization of the disklike micelles.

In the literature,[1,2] the morphologies of the aggregates from rod−coil block copolymers in solutions were observed from solution-cast films on substrates using POM and electron microscopy. In this study, the solution characteristics of the micellar structures were directly observed in solutions using POM. This is enabled by the relatively large size of the micelles (0.9 μm based on light scattering) and the optical anisotropy of the PHIC block. In Figure 11, we show a typical image that was observed under the microscope ($w = 0.004$). Bright aggregates of uniform size were found to be rotating and diffusing in and out of the plane of focus of the microscope. In most cases, snapshots of the aggregates appeared to be cylinder-like with widely varying cross sections. This apparent polydispersity is probably related to the projections of the disklike aggregates in the plane of view. In a few cases, when we observed flat disklike structures in the plane of view, their diameter was about 1−2 μm (see Figure 11). For randomly oriented disks undergoing Brownian motion, the probability of the plane of the disk coinciding with the plane of observation is extremely low. Thus, most of the time the aggregates would appear cylinder-like. The exact dimensions of the aggregate were difficult to determine due to their motion. However, the visual observed length scales are not very different from our conclusions based on light scattering (about 1 μm).

The aggregation behavior of this PHIC-*b*-PEG copolymer in toluene was further investigated by converting the PHIC block from the helix to the coil configuration to obtain a PHIC-*b*-PEG coil−coil block copolymer. Poly(*n*-alkyl isocyanates) are reported to undergo a cooperative helix−coil phase transition in solutions induced by pentafluorophenol (PFP).[31] Chemical chain scission is not involved in the transition. We added excess PFP to our PHIC-*b*-PEG/toluene solution (mole ratio of PFP to the monomer HIC was 70) to ensure complete conversion of the helices to coils. When such a solution ($w = 0.004$) was studied by POM, no structure was observed. The aggregation phenomena that we have studied are thus intimately dependent on the helical (or rodlike) nature of the well-solvated PHIC block.

Conclusions

Aggregation of an amphiphilic rod−coil diblock copolymer, poly(*n*-hexyl isocyanate)-*b*-poly(ethylene glycol) (PHIC-*b*-PEG), in toluene, a selective solvent for the rod block, was studied by light scattering. In the concentration range of $w < 0.01$, planar disklike micelles with 0.9 μm diameter and 20 nm thickness are consistent with both SLS and DLS measurements. Planar aggregates are expected if nematic interactions between the rodlike moieties in the corona are dominant. A sudden decrease in the diffusion coefficient, seen when $w > 0.01$, is attributable to nematic ordering of the micelles. The optical anisotropy of the PHIC block enables direct observations of the micelles in solution by polarized optical microscopy. The size of the aggregate observed under the microscope is comparable to that inferred from light scattering.

Acknowledgment. Financial support provided by the National Science Foundation (DMR-9901951) and the Dreyfus Foundation is gratefully acknowledged.

References and Notes

(1) Jenekhe, S. A.; Chen, X. L. *Science* **1998**, *279*, 1903; **1999**, *283*, 372.
(2) Cornelissen, J. J. L. M.; Fischer, M.; Sommerdijk, N. A. J. M.; Nolte, R. J. M. *Science* **1998**, *280*, 1427.
(3) Chen, J. T.; Thomas, E. L.; Ober, C. K.; Mao, G. P. *Science* **1996**, *273*, 343.

(4) Radzilowski, L. H.; Wu, J. L.; Stupp, S. I. *Macromolecules* **1993**, *26*, 879.
(5) Radzilowski, L. H.; Stupp, S. I. *Macromolecules* **1994**, *27*, 7747.
(6) Widawski, G.; Rawiso, M.; Francois, B. *Nature (London)* **1994**, *369*, 387.
(7) Semenov, A. N.; Vasilenko, S. V. *Sov. Phys. JETP* **1986**, *63*, 70.
(8) Semenov, A. N. *Mol. Cryst. Liq. Cryst.* **1991**, *209*, 191.
(9) Halperin, A. *Macromolecules* **1990**, *23*, 2724.
(10) Halperin, A. *Europhys. Lett.* **1989**, *10*, 549.
(11) Williams, D. R. M.; Fredrickson, G. H. *Macromolecules* **1992**, *25*, 3561.
(12) Raphael, E.; de Gennes, P. G. *Makromol. Chem. Macromol. Symp.* **1992**, *62*, 1.
(13) Clough, S. B. In *Characterization of Materials in Research Ceramics and Polymers*; Burke, J. J., Weiss, V., Eds.; Syracuse University Press: Syracuse, NY, 1975; pp 417−436.
(14) Berger, M. N. *J. Macromol. Sci., Rev. Macromol. Chem.* **1973**, *C9* (2), 269.
(15) Bur, A. J.; Fetters, L. J. *Chem. Rev.* **1976**, *76*, 727.
(16) Guenet, J. M.; Jeon, H. S.; Khatri, C.; Jha, S. K.; Balsara, N. P.; Green, M. M.; Brulet, A.; Thierry, A. *Macromolecules* **1997**, *30*, 4590.
(17) Troxell, T. C.; Scheraga, H. A. *Macromolecules* **1971**, *4*, 528.
(18) Wu, J.; Pearce, E. M.; Kwei, T. K. *Macromolecules* **2001**, *34*, 1828.
(19) Berne, B. J.; Pecora, R. *Dynamic Light Scattering*; Wiley: New York, 1976.
(20) Chu, B. *Laser Light Scattering*; Academic Press: New York, 1991.
(21) Provencher, S. *Makromol. Chem.* **1979**, *180*, 201.
(22) Schmueli, U.; Traub, W.; Rosnheck, K. *J. Polym. Sci., Part A-2* **1969**, *7*, 515.
(23) Fetters, L. J.; Yu, H. *Macromolecules* **1971**, *4*, 385.
(24) Berger, M. N.; Tidswell, B. M. *J. Polym. Sci., Part C* **1973**, *42*, 1063.
(25) Zhao, J. Q.; Pearce, E. M.; Kwei, T. K.; Jeon, H. S.; Kesani, P. K.; Balsara, N. P. *Macromolecules* **1995**, *28*, 1972.
(26) Fetters, L. J.; Balsara, N. P.; Huang, J. S.; Jeon, H. S.; Almdal, K.; Lin, M. Y. *Macromolecules* **1995**, *28*, 4996.
(27) Balsara, N. P.; Fetters, L. J. *Macromolecules* **1999**, *32*, 5147.
(28) Perrin, F. *J. Phys. Radium* **1934**, *5*, 497; **1936**, *7*, 1.
(29) Wang, Z. G.; Safran, S. A. *J. Chem. Phys.* **1988**, *89*, 5323.
(30) de Gennes, P. G.; Prost, J. *The Physics of Liquid Crystals*; Clarendon Press: New York, 1993.
(31) Fetters, L. J. *Polym. Lett.* **1972**, *10*, 577.

MA011502F